

The Effect of Machining Parameters and Drill Point Angle on the Temperature Distribution in AISI 304 Stainless Steel During Dry Drilling Operation

Amjed M. Kadhim^{1,*}, Abdulkareem F. Hassan², Qais A. Rishack³

^{1,2} Department of Mechanical Engineering, College Engineering, University of Basrah, Basrah, Iraq

³ Department of Material Engineering, College Engineering, University of Basrah, Basrah, Iraq

E-mail addresses: pgs2339@uobasrah.edu.iq, abdulkareem.flaih@uobasrah.edu.iq, qais.rashck@uobasrah.edu.iq

Received: 15 July 2021; Accepted: 2 September 2021; Published: 5 October 2021

Abstract

In this research work, the influence of cutting parameters and drill point angle on the temperature distribution in dry drilling of stainless steel AISI 304 was numerically investigated by using FE method based on DEFORM-3D V.11 commercial software. Two cutting tools of 10 mm diameter but different in point angles, one is 110° and the other is 118°. These tools were imported from specific website in a format of STL and inserted in the program during modeling of cutting tools. The material of the cutting tools is selected as high-speed steel. The workpiece model is created as cylindrical shape with 50 mm diameter and 5 mm thickness. The cutting parameters are selected as three cutting speeds (100, 200, and 300) rpm, with three feed rates (0.15, 0.25, and 0.35) mm/rev. The depth of hole is fixed for all simulations (3 mm). The percentage of increase or decrease in the resulted temperature according to the various cutting parameter was also calculated and discussed. The best cutting performance of tools according to the change of point angles was also investigated. The results provided a significant influence of cutting speed and tool point angle on the temperature generated in the machined models and very small influence of feed speed on the workpiece temperature.

Keywords: Drilling, FE Method, Deform-3D, AISI 304, High Speed Steel, Speed, Feed Rate, Tool Point Angle.

© 2021 The Authors. Published by the University of Basrah. Open-access article.

<http://dx.doi.org/10.33971/bjes.21.3.3>

1. Introduction

Drilling operation occupies an important place among all cutting operations. Drill bits are used in manufacturing due to the various dimensions, geometries, and properties. Drilling performance, economy, and surface quality of the machined hole are especially depended on the quality and type of drill bit. The factors that influence the cutting tools and properties of machined parts such as heat generated, tool life limitations must be widely studied so as to improve the performance of cutting operations and drilling operation in particular.

Ozcelik and Bagci [1] studied the influences of drilling parameters on the tool temperature during drilling operation by inserting standard thermocouples through the coolant's holes of 10 mm diameter coated carbide tools. The tool temperature went up with increasing of speed. Zeilmann and Weingaertner [2] studied the temperature generated in drilling of titanium alloy Ti-6Al-4V by using four carbide tools. The objective was to measure the temperature generated with MQL and to estimate the influence of lubrication on temperature initiated during the drilling of this alloy. Li and Salih [3] tried to calculate the tool temperature in drilling of titanium by using embedded thermocouples on the flank face of the drill tip and there was 3D finite element model used to validate the experimental model. Wu and Han [4] executed an analytical model to calculate the drilling temperature by using manual thermocouple method which was positioned at the surrounding

of the workpiece. HSS tools were used in the drilling tests. Ti-6Al-4V and AISI 1045 were used as machined materials. The temperature of Ti-6Al-4V was higher than the temperature of AISI 1045 because the thermal conductivity of first specimen is lower than the second specimen. Muhammad et al. [5] executed a 3D finite element model to study the influence of cutting parameters on temperature generated in drilling process by FE analysis software and the experiments were carried out to confirm the FE results, also the influence of friction on chip shape was studied by FE analysis. Gao et al. [6] studied the drilling method of stainless steel based on Deform-3D. They studied cutting temperature and cutting forces numerically also the effect of feed rate on cutting forces during the process. Also, the tool wear and drilling temperature were investigated. NEDIĆ and ERIC [7] measured the drill bit temperature during drilling by inserting thermocouples through the holes along the working length of the tool. Two types of workpiece materials DIN 36CrNiMo4 and 9SMn28 were used with the same cutting parameters. Su et al. [8] invented a 3D finite element model in drilling of Ti-6Al-4V alloy using DEFORM 3D software for studying of the influence of cutting parameters on force, torque and maximum drill temperature. Ucum and Kaplan [9] investigated the determination of tool wear and chip formation in drilling of AISI 1045 by using HSS tools. Berkani et al. [10] did experimental and numerical study on dry turning of AISI 304

stainless steel to check the machinability of the material by using four coated carbide cutting tools and the numerical study was done by using ANOVA software. Vas et al. [12] studied the influence of drilling parameters on tool temperature experimentally during drilling of AISI 304 with and without cooling by using tools of different point angles of 82°, 100°, and 118° and the drill bit temperature was measured by infrared thermometer. Ajayi et al. [13] included of experimental investigation and FE simulation to compute the tool-chip temperature during cutting of mild steel based on lathe machine and carbide tool. The temperature went up with increase of speed, feed rate and depth of cut. Patne et al. [14] studied the temperature distribution during drilling of titanium which included analytical, numerical and experimental study. The temperature was measured by using thermal camera and the drill bit temperature was measured by using thermocouple placed on the flank surface of the drill in experimental study. Then, the experimental and numerical studies were compared between each other for validation. The results showed that the increase of cutting speed resulted in increasing of tool and workpiece temperatures. Lazoglu et al. [15] studied the temperature in drilling of titanium alloy Ti-6Al-4V by analytical and FE modeling. Nagaraj et al. [16] made dry drilling operations of Nimonic C-263 alloy by using tungsten carbide coated tool and the temperature distribution of the cutting tool was simulated by Deform-3D software under dry drilling and the Altair AcuSolve software under cooling condition by using silver nano coolant which has great heat reduction. Uçak, and Çiçek [17] studied the effects of drilling conditions on temperature in wet drilling of Inconel 718 by numerical study and experimentally investigated, also the effect of cooling, lubrication and coating on machining of work material with respect of cutting temperature was also investigated. Erkan [18] did a wide study about the influence of cutting parameters on temperature, axial force, and stresses in dry simulation drilling of AISI 304 by using Deform-3D software. Sharma and Pradhan [19] investigated the influence of tool point angle on the heat generated in dry turning of AISI 1045 by using carbide cutting tools of different point angles as 118°, 135° and 140°. Thirukkumaran et al. [20] studied the influence of using different point angles cutting tools on the heat generated in cutting tool and workpiece materials in dry drilling of Al-5 % SiC composite as machined material and 5 mm diameter high speed steel as cutting tools with different point angles as 90°, 118°, and 135°. In the present study, the numerical simulations were carried out by using two cutting tools of different point angles of 110° and 118°, with Deform-3D V11, to study the influence of cutting parameters and drill point angle on the temperature distribution in AISI 304 during dry drilling simulations. This study is based on finite element method to measure the workpiece temperature by using many cutting speeds and feed speeds to be satisfied of evaluating all these influences on the temperature of the machined models especially the influence of drill point angle.

2. Materials

2.1. Cutting tool material

The cutting tool is the main element in drilling operation by which the chip formation and drilling performance depend on its sharpness and durability. Many tools have been invented since the early time of machining development until the moment. The cutting tool faces many aggressive conditions

during metal cutting such as tool wear, reduction of edges sharpness, high heat generation, and losing durability. The cutting tool must be created by using many hard materials, especially the materials that stand high heat and friction during metal cutting. Many attempts were executed based on experimental or analytical study to enhance the performance of drill bits such as inserting coating into the flute length of the cutting tool or using cooling methods and lubrication of the cutting area to prevent any expected loss in the lifetime of the tools due to the aggressive cutting conditions.

In this study, the material of cutting tools is high speed steel. High-speed steel tools occupy the larger place of cutting tool sales owing to its unique physical and mechanical properties that make them good candidates for the production of parts with an optimal combination of high strength, wear resistance, toughness and hardness. These tools could be used from woodworking to machining of hard materials like stainless steel, titanium based alloys, and any other high-grade alloys. A modern cutting tool was invented lately according to German classification of metals (HSS DIN 338) which has unique properties as a result of adding some important metals such as 5 % of cobalt to enhance the surface hardness. The chemical composition of HSS DIN 338 tool is mentioned in Table 1. HSS is the most material that used in manufacturing of drill bits, milling cutters, saw blades, drills, taps, broaches and more. Tools made of high speed steel permanently keep a sharp edge for longer time than other carbon steel tools, and the variety of grades and surface treatments available give options for specialized applications.

Table 1. Chemical composition of HSS DIN 338 [9].

Element	Symbol	Percentage %
Carbon	C	0.85
Silicon	Si	0.3
Manganese	Mn	0.2
Phosphor	P	0.002
Sulfur	S	0.002
Chromium	Cr	3.87
Molybdenum	Mo	4.72
Nickel	Ni	0.18
Vanadium	V	1.75
Tungsten	W	6.09
Cobalt	Co	5
Ferrous	Fe	Remaining

2.2. Workpiece material

The workpiece material is stainless steel AISI 304. This material is Fe-C alloy. Including this family, austenitic alloys are anti-corrosion materials. Stainless steel 304 is needed in factories due to its low corrosion and high mechanical properties (ultimate tensile strength is more than 590 MPa) [10]. These alloys contain more than 18 % Chromium, 8 % Nickel, and Carbon of 0.08 %, in the chemical composition [11], see Table 2 [10], and have FCC atomic structure and considered as non-magnetic alloys [10]. Stainless steel AISI 304 resists the oxidation strongly and it's impossible to be hardened through heat treatment but solution treatment or annealing can be carried out by rapid cooling after heating to 1010-1120°C. The material properties of both tool and workpiece are shown in Table 3.

Table 2. The material composition of AISI 304 [10].

Element	Symbol	Percentage %
Carbon	C	0.081
Silicon	Si	0.368
Manganese	Mn	1.74
Phosphor	P	0.018
Sulfur	S	0.019
Chromium	Cr	19.04
Molybdenum	Mo	1.24
Nickel	Ni	7.93
Ferrous	Fe	Remaining

Table 3. Material characteristics of both cutting tool and workpiece [10].

Property	AISI 304	HSS
Poisson's Ratio	0.27 - 0.3	0.3
Density	8000 kg/m ³	8138 kg/m ³
Melting Point	1450 °C	1430 °C
Elastic Modulus	193 GPa	233 GPa
Shear Modulus	77 GPa	80 - 105 GPa
Ultimate Tensile Strength	515 - 708 MPa	1280 MPa
Hardness	88 HRB 251.57 HV	62 HR
Specific Heat Capacity	500 J/kg.K	460 J/kg.K
Thermal Conductivity	16.2 W/m.K	41.5 W/m.K
Thermal Expansion	17.2 × 10 ⁻⁶ /K	12.6 × 10 ⁻⁶ /K

3. FE analysis for temperature measurement

3.1. Establishment of 3D finite element modeling

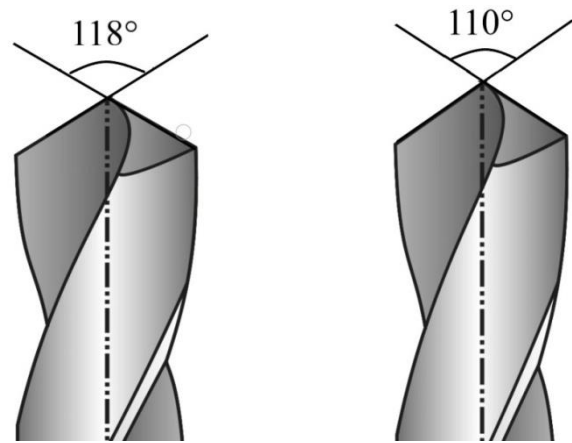
The 3D drilling has been executed by Deform-3D V11 analytical software by using FE method to make plastic deformation in the machined models and chip separation from these models. The modeling of drilling in this program passes through two stages. The first stage is preprocessing, which includes the selection of cutting parameters, initial conditions of each process, modeling of the cutting tool, modeling of the workpiece, number of simulation steps, and many other important commands. The initial conditions in preprocessing stage of modeling include environmental conditions such as temperature, and convection coefficient, and tool-workpiece interface conditions such as the factor of shear friction and the coefficient of heat transfer, see Table 4. The number of simulation steps is 2000 steps for all the simulations. The second stage of simulation is called post processing stage. In this stage, the charts and cutting temperature are provided and drilling results could be obtained. During the FE simulation, there is an option called "Deform simulation graphic", which enables to watch the running situation, the temperature level of the workpiece and in case of stop running for remeshing.

Table 4. The initial conditions of FE Modeling.

Process Condition	
1. Environment	
Temperature	25 °C
Convection Coefficient	0.02 N/sec/mm/°C
2. Tool-Workpiece Interface	
Shear Friction Factor	0.6
Heat Transfer Coefficient	45 N/sec/mm/°C

3.2. Modeling of cutting tool

Two drill bits of the same diameter and different point angle; see Fig. 1, are imported in a format of STL and inserted into the program. These tools are used in the FE simulations and considered as HSS cutting tools.

**Fig. 1** Point angles of both cutting tools.

The geometrical parameters are measured by using a special technique that is provided by the program when the tool is inserted in the modeling step, see Table 5. In the modeling of cutting tool, the decision was to ignore giving the temperature of cutting tool before drilling which means it cannot select the material of the cutting tool and no meshing technique for the cutting tool because the goal is not interested in measuring the tool temperature during drilling but to study the temperature generated in the workpiece only and the ignoring of the tool temperature measurement is helpful step because it reduces the simulation time and consider the tool as high speed steel. The neglecting of tool temperature measurement makes the program to consider these tools as high-speed steel. Only the type of the tool is allowed to be specified as "rigid" during modeling of these operations.

Table 5. Geometrical parameters of cutting tools.

Parameter	Tool 1	Tool 2
Diameter	10 mm	10 mm
Full Length	100 mm	150 mm
Flute Length	56 mm	100 mm
Shank Length	44 mm	50 mm
Shank Diameter	10 mm	10 mm
Helix Angle	28°	30°
Point Angle	110°	118°
Number of Flute	2	4
Web Thickness	1.15 mm	1.2 mm
Cutting Lip Length	5.8 mm	5.56 mm

3.3. Modeling of workpiece

The workpiece material is taken as AISI 304. The workpiece model is created as cylindrical shape with diameter of 50 mm and 5 mm thickness. During the FE process, the workpiece is motionless and the cutting tool is motivated in a rotational movement downward into the workpiece to dig out the scraping material and the process is stopped when the last step of simulation gets completed. The modeling parameters of workpiece are mentioned in Table 6.

Table 6. Modeling parameters of workpiece.

Parameter	Specification
Geometry	Cylinder
Diameter	50 mm
Thickness	5 mm
Mesh	12000
Nodes	2121
Elements	8872
Surface Polygons	2346
Mesh Size Ratio	5
Type	Plastic
Temperature	20 °C

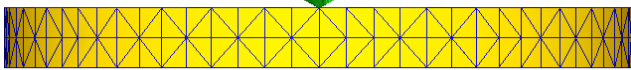
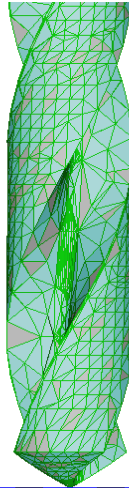


Fig. 2 The mesh model of 110° point angle drill bit and workpiece.

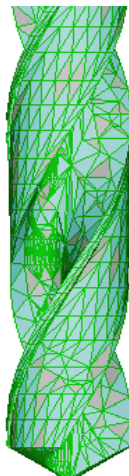


Fig. 3 The mesh model of 118° point angle drill bit and workpiece.

In the boundary condition of workpiece modeling, the motion of side and bottom surfaces of the workpiece in directions of x , y , and z is taken as zero. The target of executing such step is to confirm that the workpiece is stationary during the simulation process and the tool moving in a negative feed motion (downward) into z direction and makes a rotational movement around its axis. The restriction area which is not allowed to move is explained by red nodes during workpiece modeling, see Fig. 4.

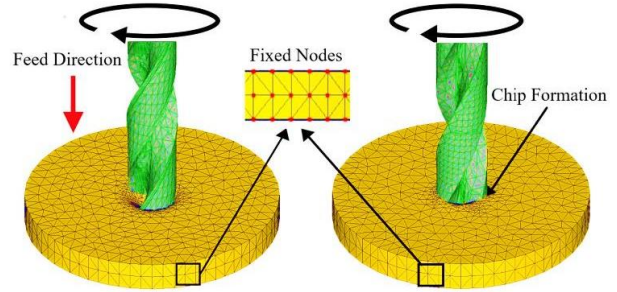


Fig. 4 The restrictions of motion in workpiece modeling.

3.4. Drilling parameters

Three spindle speeds of (100, 200, and 300) rpm with three different feed speeds of (0.15, 0.25, and 0.35) mm/rev, were used in these simulations. The drilling depth is specified for all simulations as 3 mm. Each speed is used with each feed rate which means nine drilling simulations are executed by each tool. The levels of machining parameters are explained in Table 7.

Table 7. Cutting parameters and their levels in simulations.

Factors	Unit	Levels of cutting parameters		
		1	2	3
Speed	rpm	100	200	300
Feed rate	mm/rev	0.15	0.25	0.35

4. Results and discussions

4.1. The influence of cutting speed on workpiece temperature

Figures (6), (7) and (8) discuss the variations of maximum temperature that recorded on the workpiece model with respect to cutting speed at specific feed rate. It's noted that the workpiece temperature increased noticeably with increasing of cutting speed at different feed rate and tool point angles. This result is agreed with the result reported by Thirukkumaran et al. [20], Sharma and Pradhan [19], and Vas et al. [12]. The increase of cutting speed of the tool causes excessive heat generation in the machined models at primary deformation zone (shear plane). This heat is created by the internal friction between the particles of the drilled alloy or metal as a result of chip formation at this zone by the cutting tool; see Fig. 5. The increase of cutting speed of the tool leads to increase the friction between the flank face of the cutting tool and workpiece which leads to create excessive heat at tertiary deformation zone (tool-workpiece interface), see Fig. 5. Therefore, more heat will be generated in the machined models. The increase of cutting speed of the tool leads to increase the friction between the flowing chip and the cutting tool at secondary deformation zone (chip-tool interface), see Fig. 5, which leads to rise up the frictional heat at this zone and thus more heat will be transferred to the workpiece from the secondary deformation zone. Only one process provided a drop in maximum temperature when cutting speed increased from 200 rpm to 300 rpm at feed speed of 0.15 mm/rev and 110° point angle, see Fig. 6. The percentage of increase in temperature was negative in this case, see the first point in Table 10. This is maybe due to the decrease of frictional time due to increase of cutting speed, thus less heat will be generated from friction. Such drop in temperature by increase of cutting speed was also noted when transferring from 700 rpm to 800 rpm by using 100° point angle tool in the ref. of [12].

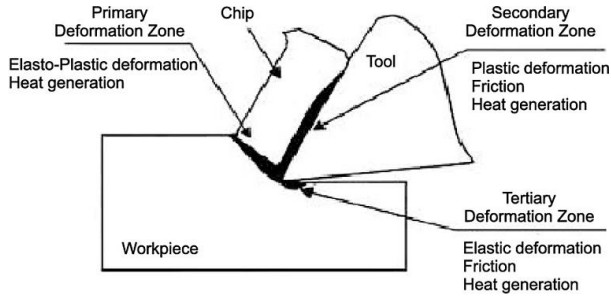


Fig. 5 The deformation zones during drilling operation which considered as sources of heat in metal cutting and drilling operation in particular [11].

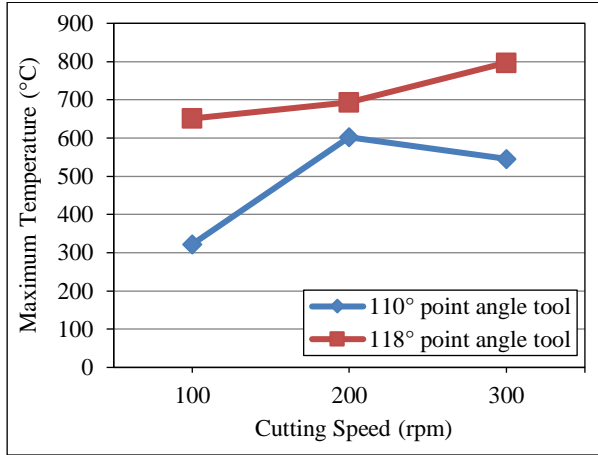


Fig. 6 The variation of temperature with respect to cutting speed at feed rate of 0.15 mm/rev.

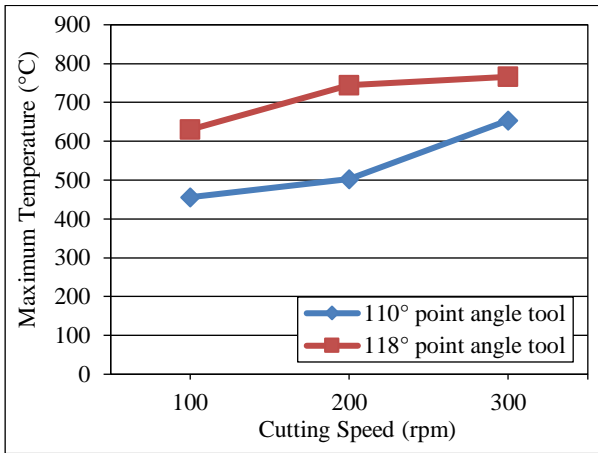


Fig. 7 The variation of temperature with respect to cutting speed at feed rate of 0.25 mm/rev.

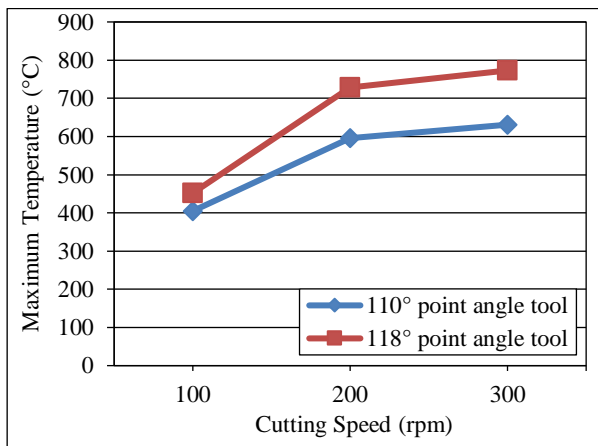


Fig. 8 The variation of temperature with respect to cutting speed at feed rate of 0.35 mm/rev.

Finally, it can be said that the increase of cutting speed causes an aggressive cutting environment which results in much heat generation in the machined model and also in the cutting tool. To calculate the percentage of increase in temperature due to the change of cutting speed, use eq. (1).

$$Percentage (\%) = \left(\frac{T_{hs} - T_{ls}}{T_{ls}} \right) 100 \% \quad (1)$$

Where, T_{hs} is the temperature at high cutting speed, and T_{ls} is the temperature at low cutting speed. Tables (8), (9) and (10) explain the percentage of increase in temperature as a result of increase in cutting speed.

Table 8. The percentage of increase in temperature due to the change of speed from 100 rpm to 200 rpm.

Test No.	Feed Rate (mm/rev)	Point angle	Max. Workpiece Temperature °C		Percentage increase in temperature (%)
			speed 100 (rpm)	speed 200 (rpm)	
1	0.15	110°	322	602	86.9
2	0.25	110°	456	503	10.3
3	0.35	110°	405	596	47.16
4	0.15	118°	651	693	6.45
5	0.25	118°	630	745	18.25
6	0.35	118°	452	729	61.28

Table 9. The percentage of increase in temperature due to the change of speed from 100 rpm to 300 rpm.

Test No.	Feed Rate (mm/rev)	Point angle	Max. Workpiece Temperature °C		Percentage increase in temperature (%)
			speed 100 (rpm)	speed 300 (rpm)	
1	0.15	110°	322	546	69.56
2	0.25	110°	456	654	43.42
3	0.35	110°	405	631	55.8
4	0.15	118°	651	797	22.4
5	0.25	118°	630	766	21.58
6	0.35	118°	452	773	71

Table 10. The percentage of increase in temperature due to the change of speed from 200 rpm to 300 rpm.

Test No.	Feed Rate (mm/rev)	Point angle	Max. Workpiece Temperature °C		Percentage increase in temperature (%)
			speed 200 (rpm)	speed 300 (rpm)	
1	0.15	110°	602	546	- 9.3
2	0.25	110°	503	654	30
3	0.35	110°	596	631	5.87
4	0.15	118°	693	797	15
5	0.25	118°	745	766	2.8
6	0.35	118°	729	773	6

4.2. The influence of feed rate on workpiece temperature

The pattern of temperature variation due to the variation of feed rate at specific cutting speed is not obvious and needs for many explanations. Figures (9), (10) and (11) show the temperature change with respect to feed rate at specific cutting speed. It's noted that the effect of feed rate cannot be considered in a positive direction with temperature because sometimes the maximum temperature goes up with increase of feed rate and sometimes the maximum temperature goes down when higher feed rate is used. According to the results of the previous researches, this pattern of temperature variation due to the change of feed rate can be concluded in the following points:

1. The increase of feed rate leads to decrease of the cutting time; thus, the frictional time will be less and then less heat generation from friction at chip-tool and tool-workpiece interfaces which means less heat will be generated and transferred to the workpiece. That's why high temperature drop was found when using larger feed rate.
2. The increase of feed rate leads sometimes to increase the thickness of un-deformed chip and thus more heat will be generated at primary deformation zone at shear plane. This is a reason for making the temperature higher when using higher feed rate. Also, the increase of feed rate causes a big forcing between the tool and the workpiece which makes high friction at tool-workpiece interface and high temperature generated in the workpiece.
3. The largest drop in temperature is found when transferring of feed from 0.15 mm/rev to 0.35 mm/rev, at speed of 100 rpm and tool of 118° point angle and the noticeable rise of temperature was found when transferring of feed rate from 0.15 mm/rev to 0.25 mm/rev, at speed of 100 rpm and tool of 110° point angle, see Fig. 9. Such drop and rise is found with the reporting results of references [12], [20].
4. The results of feed rate gave a random pattern of change in temperature with feed rate. When the tool is larger point angle, the big drop was found in temperature with increase of feed rate, and when the tool is lower point angle, there was not a noticeable drop or rise in temperature owing to the change of feed rate. Such drop was also found in Vas et al. [12], in tool temperature at larger point angle tool with increase of feed rate.

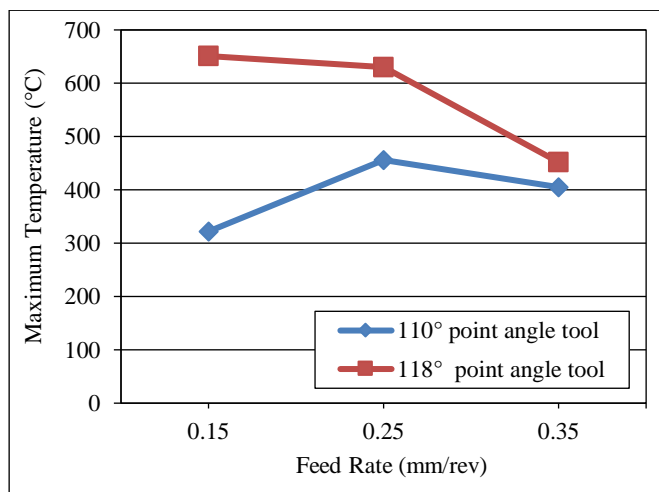


Fig. 9 The variation of temperature with respect to feed rate at speed of 100 rpm.

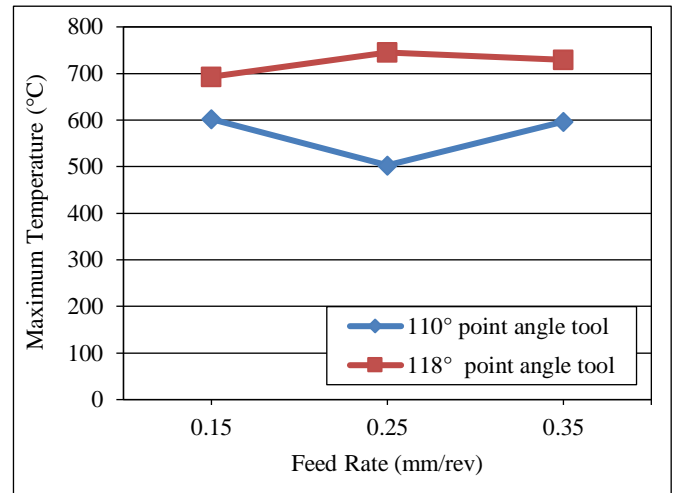


Fig. 10 The variation of temperature with respect to feed rate at speed of 200 rpm.

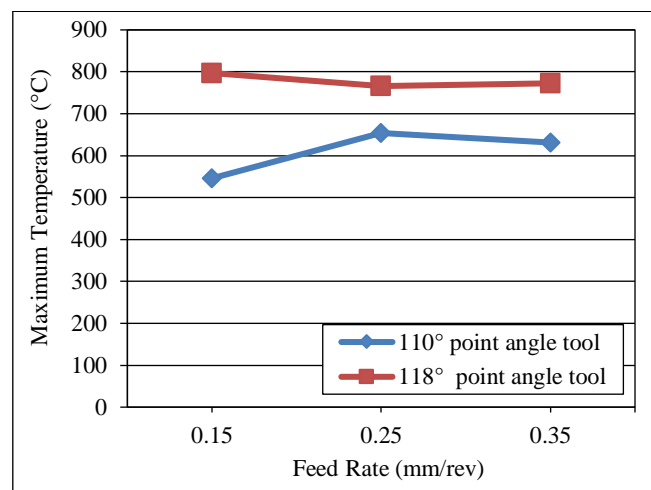


Fig. 11 The variation of temperature with respect to feed rate at speed of 300 rpm.

4.3. The influence of tool point angle on workpiece temperature

The previous figures which explain the influence of both cutting speed and feed rate on workpiece temperature referred to an extra heat which was generated by larger point angle tool. The tool of larger point angle caused higher temperatures in the machined models compared with the temperatures that caused by the smaller point angle tool, see Fig. 12. This result is agreed with Vas et al. [12], and Sharma and Pradhan [19]. In spite of little difference in point angle between tools but the amount of temperatures generated by the larger point angle tool were much higher than the amount of temperatures produced by the smaller point angle tool. This emphasized on the larger point angle cutting tool produced more friction at chip-tool interface as well as wide surface contact at tool-work model interface thus generating higher temperatures in the machined models. The increase of drill bit point angle makes the surface area of deformation or contact surface between the drill bit and the specimen wider than the drilling with less point angle tool. Thus, much friction between the flank surface of the cutting tool and the workpiece. Also, the decrease of tool point angle causes low friction at tool-chip interface, thus less heat will be generated at secondary shear zone and therefore less heat will be transferred from this zone to the workpiece.

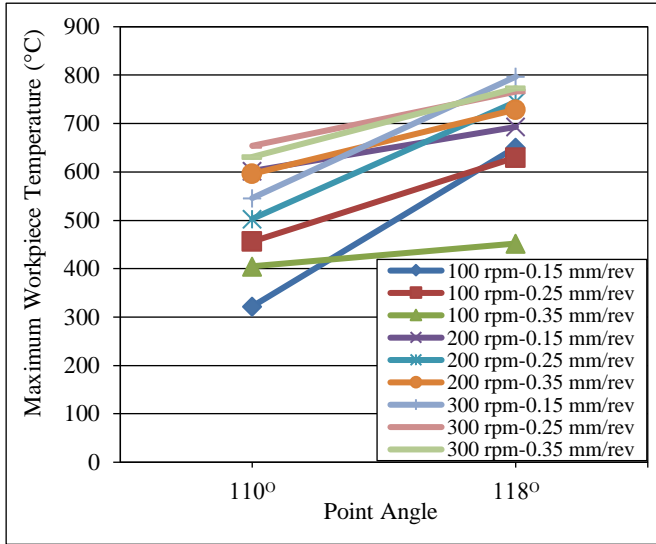


Fig. 12 The variation of workpiece temperature vs. point angle for all the simulations of different cutting parameters.

By chance, it was found out that the deformation areas on the machined models when the required depth is achieved are different between tools. This difference can be considered as the main responsible factor for changing the values of temperatures in the machined models. The deformation area was found as a conical shape for both tools, see Fig. 13. There were some parameters which needed to be measured for both deformations. The slant heights and radiuses of conical shape were measured by special measuring technique of the program, see Table 11, and then inserted in the equation (2).

$$A(\text{mm}^2) = \pi (RL + R^2) \tag{2}$$

Table 11. Slant height and radius of both deformation areas.

Parameter	Deformation of 110° point angle tool	Deformation of 118° point angle tool
Radius (R)	4.5 mm	5.5 mm
Slant height (L)	5.4 mm	6.265 mm

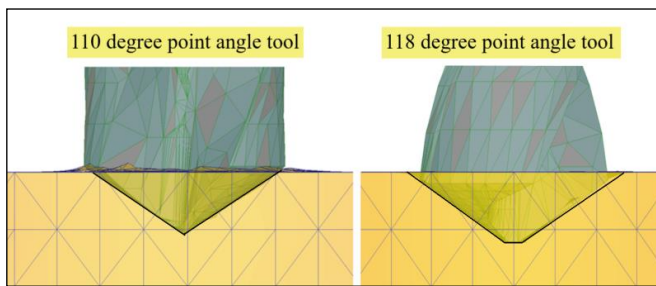


Fig. 13 The deformation areas of both tools into the work models.

The deformation area was 203.18 mm² when using 118° point angle tool and the deformation area when using 110° point angle tool was 140 mm². Thus, the area of deformation when using the largest point angle tool is larger than the one when using the smaller point angle tool. That's why we found high temperatures in drilling by the larger point angle cutting tool because of the increase of the frictional contact between the tool and workpiece. Also, the best penetration of the tool into the workpiece models was noted when the tool of larger point angle 118° was used. This can be checked by noting

Fig. 13, which shows the tool of larger point angle archives the required depth noticeably than the tool of lower point angle. This indicates that the workpiece material needs for larger point angle tool to be drilled peacefully and perfectly because such material is considered as very hard to machine and has a strong surface hardness.

To calculate the percentage of increase in temperature due to increase of point angle of the tool, use the below expression and the results inserted in Table 12.

$$\text{Percentage (\%)} = \left(\frac{T_{hp} - T_{lp}}{T_{lp}} \right) 100 \% \tag{3}$$

Where T_{hp} is the temperature when the tool is 118° point angle and T_{lp} is the temperature when the tool is 110° point angle.

Table 12. The percentage of increase in cutting temperature due to the change of point angle.

Test No.	Speed (rpm)	Feed Rate (mm/rev)	Max. Workpiece Temperature °C		Percentage increase in temperature (%)
			110° point angle tool	118° point angle tool	
1	100	0.15	322	651	102.17
2	100	0.25	456	630	38.15
3	100	0.35	405	452	11.6
4	200	0.15	602	693	15.12
5	200	0.25	503	745	48.11
6	200	0.35	596	729	22.3
7	300	0.15	546	797	45.97
8	300	0.25	654	766	17.12
9	300	0.35	631	773	22.5

5. Conclusions

The present study discusses the effect of drilling parameters such as spindle speed and feed rate on the temperature generated in workpiece of AISI 304 stainless steel during dry drilling simulations that based on FE analysis. The influence of cutting tool point angle on workpiece temperature was also investigated. The following points of conclusion have been drawn from this study:

1. The workpiece temperature is found to increase significantly with increase of cutting speed when using both tools of different point angle.
2. The best drilling performance was found when using larger point angle tool than the smaller point angle tool because the machining of such hard material like AISI 304 needs for using larger point angle tool to stand the aggressive cutting conditions like the hardness of machined models, cutting forces, and temperatures.
3. The maximum temperature rise (797° C) is found when the cutting speed is 300 rpm, feed speed is 0.15 mm/rev and tool is 118° point angle. The little temperature rise (322 °C) is found when speed is 100 rpm, feed is 0.15 mm/rev, and tool is 110° point angle. This is obvious evidence about the significant role of cutting speed and point angle in controlling of the amount of temperature that generated on the machined models.

4. The higher percentage of increase in workpiece temperature owing to the increase of cutting speed is 86.9 %, when transferring from 100 rpm to 200 rpm at feed rate of 0.15 mm/rev and tool is 110° point angle. The higher percentage of increase in workpiece temperature owing to the increase of point angle is 102.17 %, when transferring from 110° to 118° point angle, at speed of 100 rpm, and feed rate of 0.15 mm/rev. This means that the influence of point angle larger than the influence of the speed on the amount of maximum temperature generated in the machined models.
5. The cutting tool of larger point angle caused a larger damage area than the damage area that caused by the lower point angle tool. This is actually because tool of larger point angle causes a conical shape deformation which has larger radius than the radius of deformation that caused by the smaller point angle cutting tool.
6. The influence of feed rate on the temperature generated in the workpiece was not obvious enough because sometimes the temperatures went up with increase of feed rate and sometimes the temperatures dropped significantly with increase of feed rate. The larger drop in workpiece temperature was occurred when using 118° point angle cutting tool when transferring from lower to higher values of feed rate at speed of 100 rpm.

Nomenclature	
Symbol	Description
T_{hs}	Maximum workpiece temperature at higher cutting speed.
T_{ls}	Maximum workpiece temperature at lower cutting speed.
A	Area of deformation zone that caused by both tools.
R	Radius of the conical shape of deformation.
L	Slant height of the conical shape of deformation.
T_{hp}	Maximum workpiece temperature at larger point angle.
T_{lp}	Maximum workpiece temperature at smaller point angle.

References

- [1] B. Ozcelik, and E. Bagci, "Experimental and numerical studies on the determination of twist drill temperature in dry drilling: A new approach", *Materials and Design*, Vol. 27, Issue 10, pp. 920-927, 2006. <https://doi.org/10.1016/j.matdes.2005.03.008>
- [2] R. P. Zeilmann, and W. L. Weingaertner, "Analysis of temperature during drilling of Ti6Al4V with minimal quantity of lubricant", *Journal of materials processing Technology*, Vol. 179, Issue 1-3, pp. 124-127, 2006. <https://doi.org/10.1016/j.jmatprotec.2006.03.077>
- [3] R. Li, and A. J. Shil, "Tool Temperature in Titanium Drilling", *Journal of Manufacture Science and Engineering*, Vol. 129, Issue 4, pp. 740-749, 2007. <https://doi.org/10.1115/1.2738120>
- [4] J. Wu, and R. Han, "An Analytical Evaluation of Drilling Temperature", *Key Engineering Materials*, Vol. 407-408, pp. 400-403, 2009. <https://doi.org/10.4028/www.scientific.net/KEM.407-408.400>
- [5] R. Muhammad, N. Ahmed, Y. M. Shariff, and V. V. Silberschmidt, "Effect of cutting conditions on temperature generated in drilling process: A FEA approach", *Advanced Materials Research*, Vol. 223, pp. 240-246, 2011. <https://doi.org/10.4028/www.scientific.net/AMR.223.240>
- [6] X. Gao, H. Li, Q. Liu, P. Zou, and F. Liu, "Simulation of Stainless Steel Drilling Mechanism Based on Deform-3D", *Advanced Materials Research*, Vol. 160-162, pp. 1685-1690, 2011. <https://doi.org/10.4028/www.scientific.net/AMR.160-162.1685>
- [7] B. P. Nedić, and M. D. Erić, "Cutting Temperature Measurement and Material Machinability", *Thermal Science*, Vol. 18, Issue 1, pp. 259-268, 2014. <https://doi.org/10.2298/TSCI120719003N>
- [8] Y. Su, D. D. Chen, and L. Gong, "3D Finite Element Analysis of Drilling of Ti-6Al-4V Alloy", *International Conference on Computer Information Systems and Industrial Applications*, 2015. <https://doi.org/10.2991/cisia-15.2015.245>
- [9] I. Uzun, and S. Kaplan. "Determination of Tool Wear and Chip Formation in Drilling Process of AISI 1045 Material Using Plasma-Nitrided High-Speed Steel Drill Bits", *Proceedings of the Institution of Mechanical Engineers, Part B: Journal of Engineering Manufacture*, Vol. 231, No. 10, pp. 1725-1734, 2017. <https://doi.org/10.1177/0954405415608105>
- [10] S. Berkani, M. A. Yaltese, L. Boulanouar, and T. Mabrouki, "Statistical analysis of AISI 304 austenitic stainless steel machining using Ti (C, N)/A12O3/TiN CVD coated carbide tool", *International Journal of Industrial Engineering Computations*, Vol. 6, pp. 539-552, 2015. <https://doi.org/10.5267/j.ijec.2015.4.004>
- [11] M. P. Kumar, K. Amarnath, and M. S. Kumar, "A Review on Heat Generation in Metal Cutting", *International Journal of Engineering and Management Research*, Vol. 5, Issue 4, pp. 193-197, 2015.
- [12] J. S. Vas, A. Fernandes, A. D'Souza, A. Rai, and J. D. Quadros, "Analysis of Temperature Changes During Dry Drilling of Austenitic Stainless Steel on Twist Drills Having Different Point Angles", *Journal of Mechanical Engineering and Automation*, Vol. 6, No. 5A, pp. 121-125, 2016. <https://doi.org/10.5923/c.jmea.201601.23>
- [13] O. O. Ajayi, D. A. Lawal, M. Ogbonnaya, and A. Michael, "Experimental Investigation and FE Simulation of the Effect of Variable Control on Temperature Distribution in Orthogonal Metal Cutting Process", *Procedia Manufacturing*, Vol. 7, pp. 675-681, 2017. <https://doi.org/10.1016/j.promfg.2016.12.100>
- [14] H. S. Patne, A. Kumar, S. Karagadde, and S. S. Joshi, "Modeling of temperature distribution in drilling of titanium", *International Journal of Mechanical Sciences*, Vol. 133, pp. 598-610, 2017. <https://doi.org/10.1016/j.ijmecsci.2017.09.024>
- [15] I. Lazoglu, G. Poulachon, Ch. Ramirez, M. Akmal, B. Marcon, F. Rossi, J. Outeiro, and M. Krebs, "Thermal analysis in Ti-6Al-4V drilling", *CIRP Annals*, Vol. 66, Issue 1, pp. 105-108, 2017. <https://doi.org/10.1016/j.cirp.2017.04.020>
- [16] M. S. Nagaraj, Ch. Ezhilarasan, A. J. P. Kumar, and R. Betala, "Analysis of multipoint cutting tool temperature using FEM and CFD", *Manufacturing Review*, Vol. 5, No. 16, 2018. <https://doi.org/10.1051/mfreview/2018013>

- [17] N. Uçak, and A. Çiçek, “The effects of cutting conditions on cutting temperature and hole quality in drilling of Inconel 718 using solid carbide drills”, *Journal of Manufacturing Processes*, Vol. 31, pp. 662-673, 2018.
<https://doi.org/10.1016/j.jmapro.2018.01.003>
- [18] O. Erkan, and E. Yücel, “Simulation of Drilling Process of AISI 304 Plates Using Deform-3D Software”, *5th International Symposium on Multidisciplinary Studies (ISMS)*, Ankara, Turkey, 2018.
- [19] R. Sharma, and S. Pradhan, “Review on Analysis of Variation of Temperature in Simulation Using Deform-3D”, *Journal of Emerging Technologies and Innovative Research*, Vol. 6, Issue 1, pp. 1749-1755, 2019.
<http://www.jetir.org/papers/JETIRDY06279.pdf>
- [20] K. Thirukkumaran, M. Menaka, C. K. Mukhopadhyay, and B. Venkatraman, “A Study on Temperature Rise, Tool Wear, and Surface Roughness during Drilling of Al-5%SiC Composite”, *Arabian Journal for Science and Engineering*, Vol. 45, pp. 5407-5419, 2020.
<https://doi.org/10.1007/s13369-020-04427-4>